

Video Article

# Using Adeno-associated Virus as a Tool to Study Retinal Barriers in Disease

Ophélie Vacca<sup>1,2,3</sup>, Brahim El Mathari<sup>1,2,3</sup>, Marie Darche<sup>1,2,3</sup>, José-Alain Sahel<sup>1,2,3</sup>, Alvaro Rendon<sup>1,2,3</sup>, Deniz Dalkara<sup>1,2,3</sup>

<sup>1</sup>Department of Therapeutics, Institut de la Vision, Sorbonne Universités, UPMC Univ Paris 06, UMR\_S 968

<sup>2</sup>INSERM, U968

<sup>3</sup>CNRS, UMR\_7210

Correspondence to: Deniz Dalkara at [deniz.dalkara@inserm.fr](mailto:deniz.dalkara@inserm.fr)

URL: <https://www.jove.com/video/52451>

DOI: [doi:10.3791/52451](https://doi.org/10.3791/52451)

Keywords: Medicine, Issue 98, Blood-Retinal Barrier (BRB), Inner Limiting Membrane (ILM), Adeno-Associated Virus (AAV)

Date Published: 4/19/2015

Citation: Vacca, O., El Mathari, B., Darche, M., Sahel, J.A., Rendon, A., Dalkara, D. Using Adeno-associated Virus as a Tool to Study Retinal Barriers in Disease. *J. Vis. Exp.* (98), e52451, doi:10.3791/52451 (2015).

## Abstract

Müller cells are the principal glial cells of the retina. Their end-feet form the limits of the retina at the outer and inner limiting membranes (ILM), and in conjunction with astrocytes, pericytes and endothelial cells they establish the blood-retinal barrier (BRB). BRB limits material transport between the bloodstream and the retina while the ILM acts as a basement membrane that defines histologically the border between the retina and the vitreous cavity. Labeling Müller cells is particularly relevant to study the physical state of the retinal barriers, as these cells are an integral part of the BRB and ILM. Both BRB and ILM are frequently altered in retinal disease and are responsible for disease symptoms.

There are several well-established methods to study the integrity of the BRB, such as the Evans blue assay or fluorescein angiography. However these methods do not provide information on the extent of BRB permeability to larger molecules, in nanometer range. Furthermore, they do not provide information on the state of other retinal barriers such as the ILM. To study BRB permeability alongside retinal ILM, we used an AAV based method that provides information on permeability of BRB to larger molecules while indicating the state of the ILM and extracellular matrix proteins in disease states. Two AAV variants are useful for such study: AAV5 and ShH10. AAV5 has a natural tropism for photoreceptors but it cannot get across to the outer retina when administered into the vitreous when the ILM is intact (*i.e.*, in wild-type retinas). ShH10 has a strong tropism towards glial cells and will selectively label Müller glia in both healthy and diseased retinas. ShH10 provides more efficient gene delivery in retinas where ILM is compromised. These viral tools coupled with immunohistochemistry and blood-DNA analysis shed light onto the state of retinal barriers in disease.

## Video Link

The video component of this article can be found at <https://www.jove.com/video/52451/>

## Introduction

Müller cells are the major glial component of the retina. Morphologically, they span the retina radially and their endfeet, in contact with the vitreous, face the ILM and secrete components of the latter. The ILM is a basement membrane composed of about ten different extracellular matrix proteins (laminin, agrin, perlecan, nidogen, collagen and several heparin sulfate proteoglycans). During development, its presence is indispensable for retinal histogenesis, navigation of optic axons, and survival of ganglion cells<sup>1,3</sup>. However, ILM is unessential in adult retina and can be surgically removed in certain pathologies without causing retinal damage<sup>4</sup>. In gene therapy, this membrane becomes a physical barrier for efficient transduction of the retina using AAVs by intravitreal injection<sup>5</sup>.

Through the extensive arborization of their processes, Müller cells provide nutritional and regulatory support to both retinal neurons and vascular cells. Müller cells are also involved in the regulation of the retinal homeostasis, in the formation and maintenance of the BRB<sup>6</sup>. Tight junctions between retinal capillary endothelial cells, Müller cells, astrocytes and pericytes form the BRB. BRB prevents certain substances from entering the retina. In many diseases like diabetic retinopathy, retinal vein occlusion and respiratory diseases, hypoxia of the retina causes leakage through the BRB<sup>7-9</sup>. This rupture is associated with an increase in vascular permeability leading to vasogenic edema, retinal detachment and retinal damage.

Müller cells are tightly associated with blood vessels and the basement membrane, playing an important role in both BRB and ILM integrity. Consequently, labeling Müller glial cells is particularly relevant to the study of the physical state of these retinal barriers.

Classically, BRB permeability is measured using the Evans blue assay consisting of systemic injection of Evans blue dye, which binds non-covalently to plasma albumin. This assay measures the albumin leakage (protein of intermediate size, ~66 kDa) from blood vessels into the retina (see Protocols Section 5)<sup>10</sup>. Alternatively, the vascular leakage can be visualized by fluorescence retinal angiography attesting for leakage of fluorescein (small molecule, ~359 Da; see Protocols Section 6)<sup>11</sup>. Nevertheless, both methods allow evaluation of the BRB permeability to small molecules and proteins but they do not provide information about the ILM integrity.

Hence, to study BRB permeability, we used an AAV based method that gives information on the BRB permeability to larger molecules (e.g., AAV particles, 25 nm diameter). Indeed, our method can detect presence of AAV transgene in the blood, which would suggest that ~25 nm diameter particles would be able to infiltrate into the bloodstream. This method also provides information on the structure of the ILM and extracellular matrix proteins in pathological conditions. Two AAV variants are useful for such study: AAV5 and ShH10. Subretinally injected, AAV5 has a natural tropism for photoreceptors and retinal pigment epithelium<sup>12</sup> but it cannot get across to the outer retina when administered into the vitreous in wild-type retinas with intact ILM<sup>5,13</sup>. ShH10 is an AAV variant that has been engineered to specifically target glial cells over neurons<sup>14,15</sup>. ShH10 selectively labels Müller cells in both healthy and diseased retinas with increased efficiency in retinas with compromised barriers<sup>16</sup>. These viral tools coupled with immunohistochemistry and blood-DNA analysis provide information on the state of retinal barriers and their involvement in disease (**Figure 1**).

## Protocol

All animals used in this study were cared for and handled according to the ARVO Statement for the Use of Animals in Ophthalmic and Vision Research.

## 1. Production of Recombinant AAV (rAAV) by Transient Transfection of HEK-293 Cells<sup>17,18</sup>

NOTE: See McClure C, JoVE (2011)<sup>19</sup>.

1. Purify a large-scale plasmid preparation (at least 1 mg/ml) of the AAV vector plasmids. Use 3 plasmids. The AAV helper plasmid carrying the replication and capsid genes without the AAV inverted terminal repeats ITRs, the transgene expression cassette carrying the AAV ITR referred to as the transfer plasmid, and the plasmid supplying the adenovirus helper genes *E2*, *E4*, and *VA* RNA genes referred to as pHELPER.
2. Transfect 293 cells with these 3 plasmids using polyethyleneimine (or other transfection reagent). Above 80% of transfection efficiency is necessary for good viral yields.
3. Purify recombinant AAV from 293 cell lysates on an iodixanol gradient. 15%, 25%, 40%, and 60% iodixanol is used to obtain the gradient. Collect 40% iodixanol fraction containing AAV particles, concentrate the fraction after ultracentrifugation at 500,000 x g for 1 hr and buffer exchange against PBS (phosphate buffered saline) with 0.001% Pluronic.
4. To determine viral genomic titer<sup>20</sup>, perform a DNase ProteinaseK digest followed by QPCR. The forward and reverse primers amplify the 62 bp region located in the AAV2 ITR. For the plasmid standard, the probe is labeled with FAM and has a black hole quencher (BHQ).
5. Carry out qPCR (quantitative polymerase chain reaction) in a final volume of 25  $\mu$ l using 340 nM reverse ITR primer, 100 nM forward ITR primer, 100 nM AAV2 ITR probe, 0.4 mM dNTPs, 2 mM MgCl<sub>2</sub>, 1x Platinum Taq Buffer, 1U Platinum Taq and 5  $\mu$ l template (standard, sample and no template control).
6. For the standard, use the plasmid for transfection in 7 x 10-fold serial dilutions (5  $\mu$ l each of  $2 \times 10^9$  to  $2 \times 10^3$  genomes/ml resulting in a final concentration from  $10^{10}$  to  $10^4$  genomes/ml).
7. Begin the program by an initial denaturation step at 95 °C for 15 min followed by 40 cycles of denaturation at 95 °C for 1 min and annealing/extension at 60 °C for 1 min. Store at 4 °C for a short-term storage or at -20 °C for long storage periods.

## 2. Intravitreal Injection of AAV

1. Anesthetize C57BL6J mice with ketamine (50 mg/kg) and xylazine (10 mg/kg) and verify the loss of righting reflex, the withdrawal reflex and tail pinch response indicating a proper anesthetization. Dilate pupils by corneal application of neosynephrine 5% and mydriaticum 0.5% eye drops. Use vet ointment on eyes to prevent dryness while under anesthesia.
2. Pass an ultrafine 30 G disposable needle through the equator and next to the limbus, into the vitreous cavity (see Chiu K, JoVE (2007)<sup>21</sup>). Inject 1  $\mu$ l stock containing  $1$  to  $4 \times 10^{11}$  vp of ShH10-GFP or AAV5-GFP with direct observation of the needle in the center of the vitreous cavity (**Figure 1**). Use one eye as a control for ILM experiments. Inject both eyes for BRB experiments. Apply an anti-inflammatory and antibacterial topical treatment on injected eyes.
3. Dilate pupils with neosynephrine and mydriaticum eye drops for imaging. Perform fundus examinations with an eye fundus camera to follow GFP (Green Fluorescent Protein) expression 1 week, 2 weeks, 1 month, and 2 months after intravitreal injection (**Figure 1**). Sacrifice mice by CO<sub>2</sub> inhalation 1 to 2 months post-injection.

## 3. Immunohistochemistry

1. For retinal cryosections (**Figure 1**), dissect enucleated eyes to remove lens and cornea, and immersion fix in 4% paraformaldehyde for 1 hr.
  1. Cryoprotect the previously fixed eyes in 10% sucrose for 1 hr at room temperature, 20% sucrose for another hr at room temperature. Cryoprotect in 30% sucrose solution, overnight at 4 °C. Freeze and embed eyecups in embedding resin such as Cryo-matrix. Make 10  $\mu$ m cryosections and mount on slides specially treated for frozen tissue sections and that improve tissue adherence during staining.
  2. Permeabilize sections with 0.1% Triton X100 in PBS pH 7.4 for 5 min. Wash 2x in PBS and block for 1 hr at room temperature in PBS with 1% BSA, 0.1% Tween 20.
2. For retinal flatmounts (**Figure 1**), fix enucleated eyes in 4% paraformaldehyde for 15 min to facilitate the dissection.
  1. In 15-30 min, dissect the eyes to remove the cornea and lens. Separate the retina from the retinal pigment epithelium (RPE) and sclera by cutting around the ora serrata and the optic nerve. Immerse in 4% paraformaldehyde for another 30 min to fix the retina and the fluorescent protein in transduced retinal cells (fixation must not exceed 24 hr). Wash 5 min in sterile PBS, pH 7.4.
  2. Change the PBS to blocking buffer (PBS with 1% BSA, 2% normal goat or donkey serum, 0.5% Triton X-100), and incubate in blocking buffer for either 4 hr at room temperature or 4 °C overnight.
3. Incubate tissues with primary antibodies in blocking buffer for either 4 hr at room temperature or at 4 °C overnight. Wash 3x with PBS.

NOTE: The antibodies used are as follows: anti-laminin (1/1,000) labeling the ILM, anti-rhodopsin clone 4D2 (1/500) labeling rods, anti-glutamine synthetase clone GS-6 (1/1,500) labeling Müller cells, PNA Lectin (1/40) labeling cones.

4. Incubate tissues with 1:500 dilution of alexa fluor conjugated secondary antibodies in blocking buffer for 1 hr (cryosections) or 2 hr (flatmounts) at room temperature and protected from light. Wash 3x with PBS.
5. Make relieving cuts to the retina and flatmount it onto a glass slide with either the photoreceptor or retinal ganglion cell (RGC) side facing upwards. Add aqueous mountingmedium, apply coverslip and store at 4 °C.
6. Perform confocal microscopy on laser-scanning confocal microscope. Acquire images sequentially, line by line, to reduce excitation and emission crosstalk. Define step size according to the Nyquist–Shannon sampling theorem. Use exposure settings that minimize oversaturated pixels in the final images. Process 12-bit images with FIJI, project Z-sections on a single plane using maximum intensity under Z-project function and finally convert to 8-bit RGB color mode.

## 4. PCR Analysis of Mouse Blood Samples

1. Inject 100 µl stock containing 1 to 4 x 10<sup>11</sup> particles of an AAV-GFP into the penile vein of anesthetized C57BL6J mice (5% of isoflurane for induction in a close chamber and 2.5% of isoflurane through a nose cone during surgery) using an insulin syringe with an ultra-fine 6 mm needle. This animal will serve as a positive control of circulating AAV particles.
2. Sample blood from mouse tail before injection and 3 hr, 24 hr, 2 days, and 3 days after ShH10 intravitreal injection or after intrapenile injection (**Figure 1**). About 10-20 µl is collected in heparin tubes. Sacrifice mice by CO<sub>2</sub> inhalation after completion of the procedure.
3. Extract genomic DNA from blood samples using the extraction kit of your choice.
4. Perform PCR amplification of genomic DNA. For this protocol use the following primer pair: GFP, sense 5'-CGACACAATCTGCCCTTTCG-3', antisense 5'-CATGGACGAGCTGTACAAGGGA-3'. The following PCR program was performed: 95 °C 2 min (1 cycle); 95 °C 45 sec, 55 °C 1 min, 72 °C 45 sec (30 cycles); 72 °C 5 min (1 cycle); 4 °C hold.

## 5. Optional Evans Blue Method

NOTE: Quantify vascular permeability by measuring albumin leakage from blood vessels into the retina using the Evans blue method<sup>10</sup>.

1. Prepare Evans Blue dye by dissolution in a normal saline solution (6 mg/ml), sonication for 5 min in an ultrasonic cleaner, and filtration through a 5 µm filter.
2. Anesthetize C57BL6J mice (isoflurane inhalation, see step 4.1), check the loss of righting reflex, the withdrawal reflex and tail pinch response indicating a proper anesthetization, and inject Evans blue (45 mg/kg) through the penile vein (**Figure 1**). Check that paws, muzzle, and ears of mice become clearly blue following Evans blue injection, confirming the uptake and distribution of the dye.
3. Anesthetize C57BL6J mice 3 hr after injection of the dye with ketamine (50 mg/kg) and xylazine (10 mg/kg) and verify the loss of righting reflex indicating a proper anesthetization. Sample intracardially about 500 µl of blood in heparin tubes and perfuse mice for 2 min via the left ventricle with a citrate buffer (0.05 M, pH 3.5; dissolve 7.8 g of citric acid and 3.8 g of sodium citrate in 1 L of distilled water) pre-warmed to 37 °C to prevent vasoconstriction. Mice are sacrificed via the perfusion.
4. After perfusion, enucleate and carefully dissect both eyes under an operating microscope to collect the retinas (see Section 3.2). Dry retinas in a centrifugal evaporator overnight, weigh, and extract the Evans blue dye by incubating retinas with 100 µl of formamide for 18 hr at 65 °C with shaking (100 x g). Centrifuge retina samples in 30K omega filter tubes at 20,798.5 x g for 2 hr at 4 °C and centrifuge blood samples at 20,798.5 x g for 15 min at 4 °C.
5. Use both supernatants to measure absorbance. Determine absorbance of each sample by subtracting the absorbance maximum for Evans blue at 620 nm to the absorbance minimum at 740 nm. Calculate Evans blue concentration in plasma and retina from a standard curve of Evans blue in formamide. Express BRB permeability in microliter of Evans blue per gram of dry retina per hour (µl plasma/g retinal dry wt/hr).

## 6. Optional Fluorescein Angiography

NOTE: Leakage from retinal blood vessels in mice can be visualized by intraperitoneal injection of sodium fluorescein.

1. Anesthetize C57BL6J mice (isoflurane inhalation, see **step 4.1**) and dilate pupils with eye drops (neosynephrine and mydriaticum). Use vet ointment on eyes to prevent dryness while under anesthesia.
  2. Inject intraperitoneally 0.01-0.02 ml of 10% sodium fluorescein in 0.1 ml sterile saline for fluorescein angiography.
  3. Collect images of both eyes after injection using an eye fundus camera. Sacrifice mice by CO<sub>2</sub> inhalation after the procedure.
- NOTE: 20 sec are necessary for the retinal vessels to become visible on angiography. Images have to be captured between 3-10 min maximum after fluorescein injection. The leakage spots (if present) are observable after 2.5 min. At later time points the image quality is lost due to sodium fluorescein diffusing into the vitreous, thus only images shortly obtained after are used for analysis.

## Representative Results

We expect increased retinal transduction of Müller glial cells using ShH10 if the animal model shows perturbations in the structure of the ILM (**Figure 2A-B**). For example, we have shown that in absence of Dp71, ShH10 targets specifically but more efficiently Müller glial cells by intravitreal injection, indicating increased permeability of the ILM in this mouse line compared to wild-type mice<sup>16</sup> (**Figure 2C-F**).

AAV5 can also be used as an indicator of ILM permeability. AAV5, ineffective by intravitreal injection in wild-type mice, becomes strongly effective in gene delivery to photoreceptors in mice with compromised retinal barriers such as the Dp71-null mice<sup>16</sup> or in other retinal degenerations<sup>22</sup> (**Figure 2G-H**). This further confirms the ILM disorganization and potential permeability increase in the extra-cellular matrix surrounding the retinal neurons.

We found that, the BRB breakdown of Dp71-null mice remains selective to AAV particles since no trace of AAV were found in blood samples of intravitreally injected Dp71-null mice<sup>16</sup> (Figure 3).

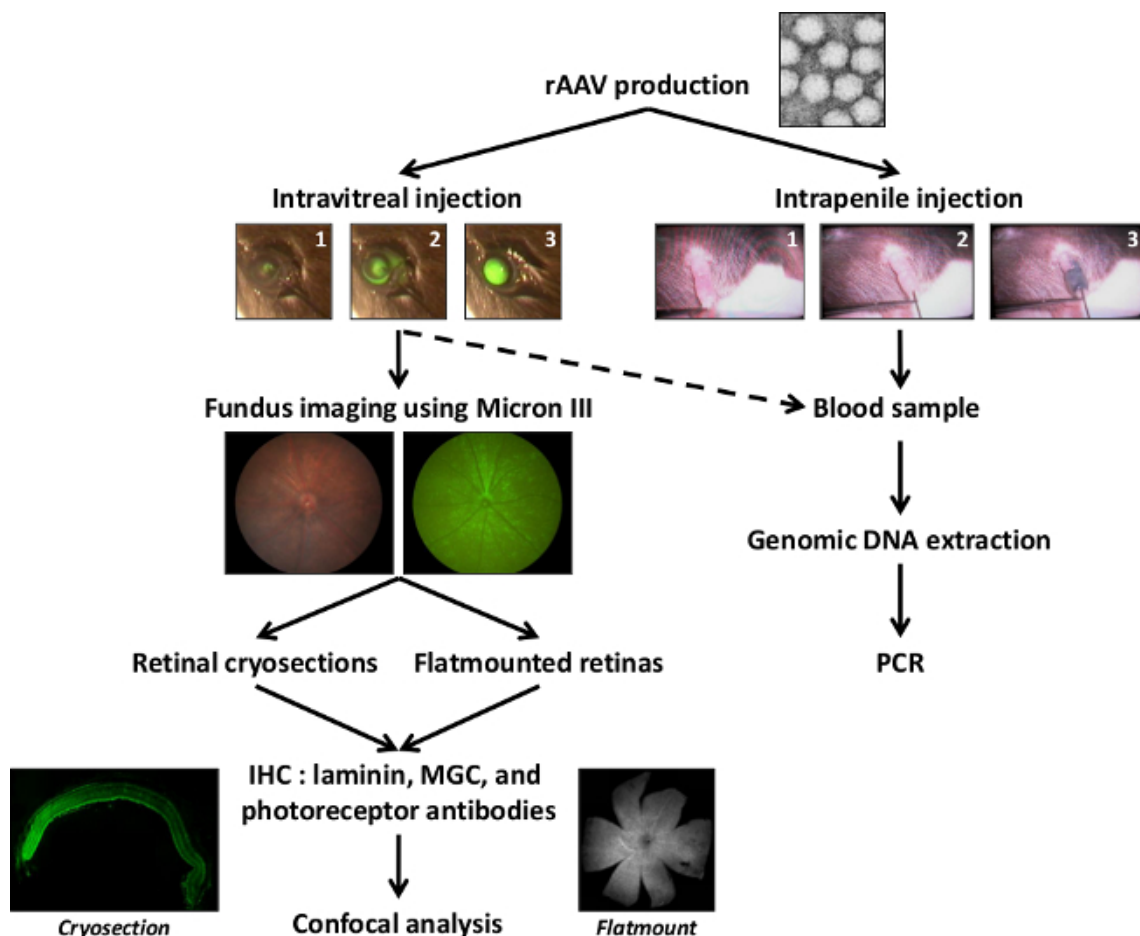


**Figure 1: Schematic representation of the general protocol.** After AAV production, particles are injected into the vitreous or into the penile vein to anesthetized adult mice. Fundus images with Micron III camera are performed to follow the GFP expression. The GFP expression pattern is analyzed on retinal cryosections and flatmounted retinas thanks to immunohistochemistry and confocal images. The AAV passage through the BRB is assessed by PCR analysis on blood samples coming from intravitreally or intraperitoneally injected mice, in order to detect the presence of GFP sequence, indicator of the AAV particles presence into the bloodstream.



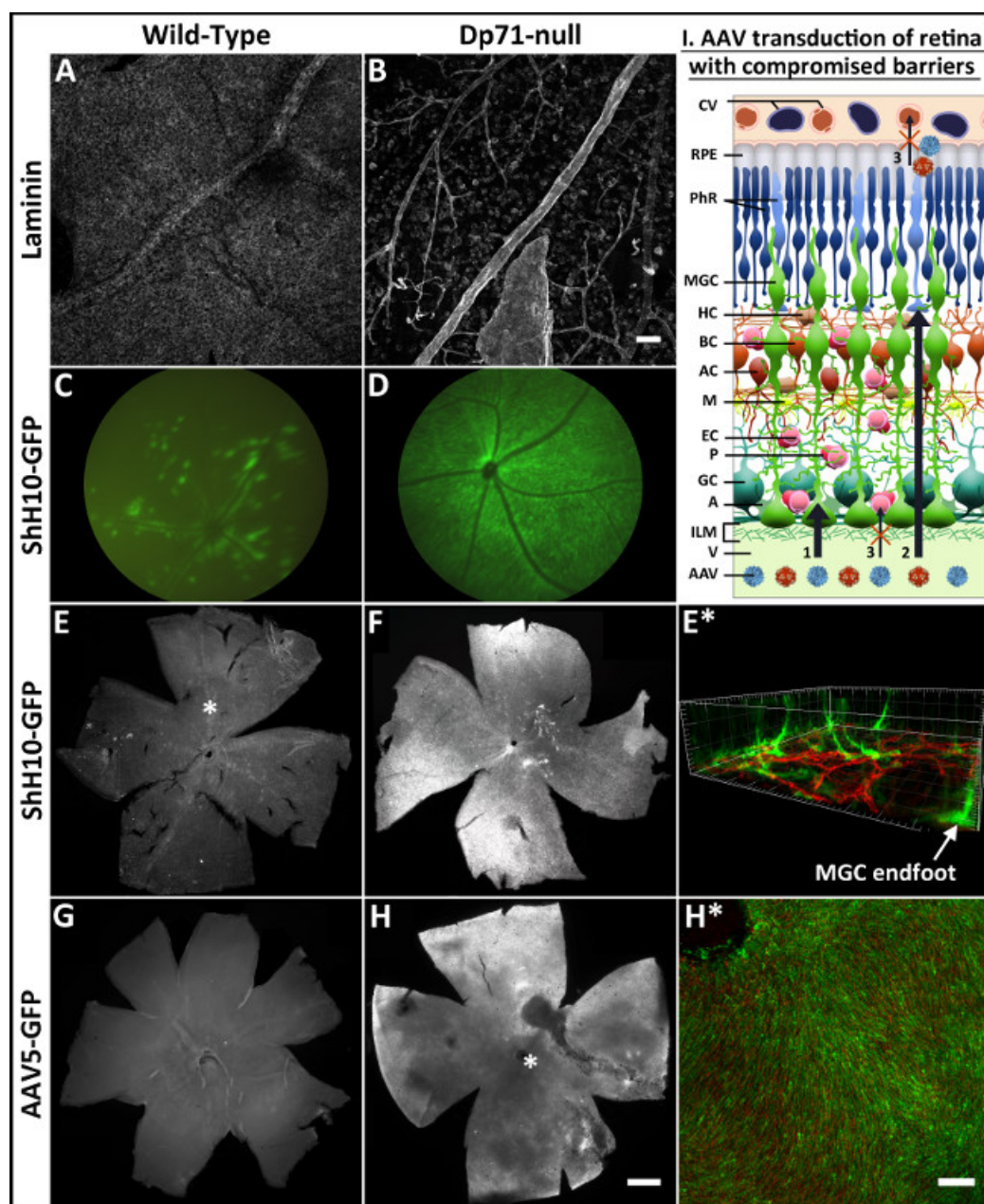


**Figure 2: ILM permeability to AAV transduction.** Confocal images of flatmounted wild-type and Dp71-null retinas labeled with a pan-laminin antibody (**A, B**) (scale bar: 50  $\mu$ m). Fundus images showing GFP expression (**C, D**). Flatmounted retinas one month after ShH10-GFP intravitreal injection (**E, F**). Three dimensional reconstruction (**E\***) of the area indicated by an asterisk in **E** showing transduced Müller glial cells in green and astrocytes in red (anti-GFAP antibody). Flatmounted retinas one month after intravitreal injection of AAV5-GFP (**G, H**) (scale bar: 500  $\mu$ m). Confocal image of the area indicated by an asterisk in **H** showing transduced photoreceptors in green and cone outer segments in red (PNA lectin staining) (**H\***). The left column shows results from wild-type mouse retinas and the middle column shows results from Dp71-null mouse retinas. The schema (**I**) represents AAV transduction of retina with compromised barriers as Dp71-null retina, through the vitreous. Abbreviations : CV, choroidal vessels; RPE, retinal pigment epithelium; PhR, photoreceptor cells (rods and cones); MGC, Müller glial cells; HC, horizontal cells; BC, bipolar cells; AC, amacrine cells; M, microglia; EC, endothelial cells; P, pericytes; GC, ganglion cells; A, astrocytes; ILM, inner limiting membrane; V, vitreous; AAV, adeno-associated virus. (Re-print with permission from Vacca *et al.*, *Glia* (2013)<sup>16</sup>, #3483740951391).

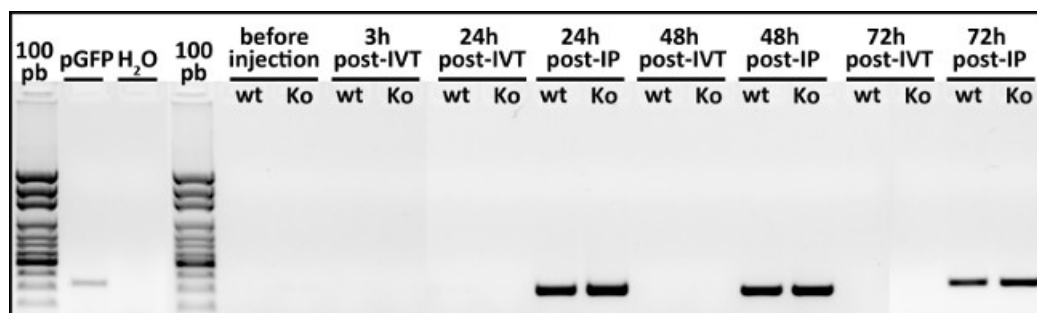


**Figure 3: BRB permeability to AAV particles.** PCR amplification of GFP transgene extracted from mouse blood samples. Mice either injected intravitreally (IVT) with ShH10-GFP or intraperitoneally (IP) with AAV-GFP at different times after injection. Lane 5-18, odd numbers for wild-type mice and even numbers for Dp71-null mice; lane 2, 1 ng of the AAV plasmid, pTR-SB-smCBA-hGFP; lane 3, water; lanes 5-6, blood DNA before injection; lanes 7-8, 3 hr post-IVT; lanes 9-10, 24 hr post-IVT; lanes 11-12, 24 hr post-IP; lanes 13-14, 48 hr post-IVT; lanes 15-16, 48 hr post-IP; lanes 17-18, 72 hr post-IVT; lanes 19-20, 72 hr post-IP. Lanes 1 and 4, Invitrogen scale ladder (100 bp): 100, 200, 300, 400, 500, 600, 700, 800, 1,000, 1,500, 2,000, 3,000 bp. (Re-print with permission from Vacca *et al.*, *Glia* (2013)<sup>16</sup>, #3483740951391).

## Discussion

The BRB regulates the exchange of molecules between blood and retina. Its breakdown is associated with various diseases such as diabetic retinopathy or age-related macular degeneration (AMD). We recently showed that in a dystrophin knock-out mouse, which displays permeable BRB, the retina becomes more permissive to gene delivery mediated by adeno-associated viral vectors (AAV). However, despite BRB permeability AAV particles injected intraocularly stay confined to the ocular compartment in this model. Our results indicate that gene therapy for diseases that display permeable BRB does not represent additional risks of systemic side effects. Furthermore, they support the fact that other barriers such as the ILM become compromised during retinal disease allowing better access to viral particles. Our findings lead us to think that AAV encoding reporter genes is an excellent tool to study BRB permeability and ILM integrity in animal models of retinal disease. Particularly, the AAV variant ShH10, which specifically labels Müller glia can be used as a tool to label retinal glia and report on the state of the retina in response to disease. ShH10 will selectively label Müller glia in both healthy and diseased retinas. However, both ShH10 and other AAVs will provide more efficient gene delivery in retinas with compromised barriers.

Some critical steps in applying the above-described protocols are (1) developing manual dexterity to perform the safest intravitreal injection, and (2) properly fixing the tissue before and after dissection. In studying retinal barriers, the intravitreal injection should be well executed that is - without touching the lens or the retina. Damaging the lens or detaching the retina influences the BRB permeability<sup>23,24</sup>. Additionally lens damage impedes fundus imaging. Touching the retina can rupture the ILM and damage the retinal structure. To avoid touching the retina, the experimenter should observe the tip of the Hamilton syringe in the middle of the vitreous cavity, in front of the retina. A non-toxic dye can be included (such as Phenol red or fluorescein) in the viral solution to aid in the observation of the fluid injection into the vitreous. Damage to the retina can be readily observed during fundus imaging following the injection procedure. Another critical step is the fixation of the tissue after sufficient expression levels are reached. After enucleation, eyes must be immediately immersed in fixative buffer and before tissue permeabilization a second fixation is necessary in order to prevent GFP leakage. It can be helpful to slit the cornea before immersing the entire eye in the fixative - this will give the fixative a chance to permeate into the vitreous. This step can increase the overall tissue stability.

Lastly, it is also important to inject enough AAV particles to transduce efficiently the retina and to observe GFP expression on eye fundus images. The optimal amount of AAV particles is about  $10^{10}$ - $10^{11}$  vg per eye, below  $10^{10}$  particles the GFP expression is not always observed by fundus imaging.

This technique will not give the possibility to directly observe the ILM or the vasculature beneath the BRB. However it provides a way to examine retinal barriers and their modification in disease states, in a way that was previously not possible using the Evans blue assay and fluorescein angiography. Using AAVs with specific retinal transduction properties, it is possible to get better insight into the state of the retina with respect to the glial cells, their extracellular matrix and ILM. After mastering this technique, one can test the efficacy of therapeutic strategies and their influence on BRB and retinal permeability and go towards a better understanding of disease progression and the possibility to restore normal conditions after treatment in a mouse model of retinal disease.

## Disclosures

The authors have nothing to disclose.

## Acknowledgements

We thank the imaging platform of the Institut de la Vision. We acknowledge the French Muscular Dystrophy Association (AFM) for a PhD fellowship to O.V. and Allergan INC. This work performed in the frame of the LABEX LIFESENSES [reference ANR-10-LABX-65] was supported by French state funds managed by the ANR. We thank Peggy Barbe, and Mélissa Desrosiers for technical assistance with AAV preparations. We are grateful to Stéphane Fouquet for excellent technical assistance in confocal microscopy and his expert input with the interpretation of the results.

## References

1. Halfter, W. Disruption of the retinal basal lamina during early embryonic development leads to a retraction of vitreal end feet, an increased number of ganglion cells, and aberrant axonal outgrowth. *J Comp Neurol*. **397** (1), 89-104, doi: 10.1002/(SICI)1096-9861(19980720)397:1<89::AID-CNE7>3.0.CO;2-E (1998).
2. Halfter, W., Dong, S., Balasubramani, M., & Bier, M. E. Temporary disruption of the retinal basal lamina and its effect on retinal histogenesis. *Dev Biol*. **238** (1), 79-96, doi:10.1006/dbio.2001.0396 (2001).
3. Halfter, W., Willem, M., & Mayer, U. Basement membrane-dependent survival of retinal ganglion cells. *Invest Ophthalmol Vis Sci*. **46** (3), 1000-1009, doi:10.1167/iops.04-1185 (2005).
4. Abdelkader, E., & Lois, N. Internal limiting membrane peeling in vitreo-retinal surgery. *Surv Ophthalmol*. **53** (4), 368-396, doi:10.1016/j.survophthal.2008.04.006 (2008).
5. Dalkara, D. *et al*. Inner limiting membrane barriers to AAV-mediated retinal transduction from the vitreous. *Mol Ther*. **17** (12), 2096-2102, doi:10.1038/mt.2009.181 (2009).
6. Bringmann, A. *et al*. Muller cells in the healthy and diseased retina. *Prog Retin Eye Res*. **25** (4), 397-424, doi:10.1016/j.preteyeres.2006.05.003 (2006).
7. Eichler, W., Kuhrt, H., Hoffmann, S., Wiedemann, P., & Reichenbach, A. VEGF release by retinal glia depends on both oxygen and glucose supply. *Neuroreport*. **11** (16), 3533-3537 (2000).
8. Kaur, C., Foulds, W. S., & Ling, E. A. Blood-retinal barrier in hypoxic ischaemic conditions: basic concepts, clinical features and management. *Prog Retin Eye Res*. **27** (6), 622-647, doi:10.1016/j.preteyeres.2008.09.003 (2008).
9. Kaur, C., Sivakumar, V., & Foulds, W. S. Early response of neurons and glial cells to hypoxia in the retina. *Invest Ophthalmol Vis Sci*. **47** (3), 1126-1141, doi:10.1167/iops.05-0518 (2006).
10. Xu, Q., Qaum, T., & Adamis, A. P. Sensitive blood-retinal barrier breakdown quantitation using Evans blue. *Invest Ophthalmol Vis Sci*. **42** (3), 789-794 (2001).
11. Amato, R., Wesolowski, E., & Smith, L. E. Microscopic visualization of the retina by angiography with high-molecular-weight fluorescein-labeled dextrans in the mouse. *Microvasc Res*. **46** (2), 135-142, doi:10.1006/mvre.1993.1042 (1993).
12. Yang, G. S. *et al*. Virus-mediated transduction of murine retina with adeno-associated virus: effects of viral capsid and genome size. *J Virol*. **76** (15), 7651-7660, doi: 10.1128/JVI.76.15.7651-7660.2002 (2002).
13. Li, W. *et al*. Gene therapy following subretinal AAV5 vector delivery is not affected by a previous intravitreal AAV5 vector administration in the partner eye. *Mol Vis*. **15** 267-275 (2009).
14. Koerber, J. T. *et al*. Molecular evolution of adeno-associated virus for enhanced glial gene delivery. *Mol Ther*. **17** (12), 2088-2095, doi:10.1038/mt.2009.184 (2009).
15. Klimczak, R. R., Koerber, J. T., Dalkara, D., Flannery, J. G., & Schaffer, D. V. A novel adeno-associated viral variant for efficient and selective intravitreal transduction of rat Muller cells. *PLoS One*. **4** (10), e7467, doi:10.1371/journal.pone.0007467 (2009).
16. Vacca, O. *et al*. AAV-mediated gene delivery in Dp71-null mouse model with compromised barriers. *Glia*. doi:10.1002/glia.22617 (2013).
17. Choi, V. W., Asokan, A., Haberman, R. A., & Samulski, R. J. Production of recombinant adeno-associated viral vectors. *Curr Protoc Hum Genet*. **Chapter 12** Unit 12 19, doi:10.1002/0471142905.hg1209s53 (2007).
18. Choi, V. W., Asokan, A., Haberman, R. A., & Samulski, R. J. Production of recombinant adeno-associated viral vectors for in vitro and in vivo use. *Curr Protoc Mol Biol*. **Chapter 16** Unit 16 25, doi:10.1002/0471142727.mb1625s78 (2007).
19. McClure, C., Cole, K. L., Wulff, P., Klugmann, M., & Murray, A. J. Production and titring of recombinant adeno-associated viral vectors. *J Vis Exp*. (57), e3348, doi:10.3791/3348 (2011).
20. Aurnhammer, C. *et al*. Universal real-time PCR for the detection and quantification of adeno-associated virus serotype 2-derived inverted terminal repeat sequences. *Hum Gene Ther Methods*. **23** (1), 18-28, doi:10.1089/hgtb.2011.034 (2012).
21. Chiu, K., Chang, R. C., & So, K. F. Intravitreal injection for establishing ocular diseases model. *J Vis Exp*. (8), 313, doi:10.3791/313 (2007).
22. Kolstad, K. D. *et al*. Changes in adeno-associated virus-mediated gene delivery in retinal degeneration. *Hum Gene Ther*. **21** (5), 571-578, doi:10.1089/hum.2009.194 (2010).
23. Sene, A. *et al*. Functional implication of Dp71 in osmoregulation and vascular permeability of the retina. *PLoS One*. **4** (10), e7329, doi:10.1371/journal.pone.0007329 (2009).
24. Benard, R. A New Quantifiable Blood Retinal Barrier Breakdown Model In Mice. ARVO Annual Meeting, poster presentation #4518/A272 (2011).